

Nanomolar fluorogenic detection of Al(III) by a series of Schiff bases in an aqueous system and their application in cell imaging†

Cite this: *Org. Biomol. Chem.*, 2014, **12**, 4445

Sanyog Sharma,^a Maninder Singh Hundal,^{*a} Amandeep Walia,^b Vanita Vanita^b and Geeta Hundal^{*a}

Received 13th February 2014,
Accepted 29th April 2014

DOI: 10.1039/c4ob00329b

www.rsc.org/obc

Three positional isomers of a Schiff base containing –OH as end groups have been synthesized and evaluated for selective Al(III) detection due to inhibition of ES IPT, PET and activation of CHEF in 70% aqueous medium. Devoid of any conventional fluorophore, these sensors have nanomolar detection limits with high quantum yields and naked eye sensing of Al(III). Moreover, these probes have been demonstrated to enable the Al(III) detection in live human HeLa cells and rat C6 glioma cells using a confocal microscope.

Introduction

Aluminium is one of the most abundant metals in the earth's crust; it finds wide applications in our daily life such as in food additives, packing materials, water treatment, paper making, colours and in some medicines.¹ The toxicity of Al(III) causes diseases such as Alzheimer's, Parkinson's disease, bone softening, impaired lung function, fibrosis, chronic renal failure, *etc.*² Moreover the concentration of aluminium has been found to be crucial for fish and also for agricultural production as it increases the acidity of the soil.³ The FAO/WHO Joint Expert Committee on food additives recommends a daily intake of Al(III) ions for the human body of 3–10 mg and a weekly intake of 7 mg kg⁻¹ body weight.⁴ Since there is a close association between Al(III) and human health, the detection of Al(III) is crucial in controlling its concentration in the biosphere. Among various sensing techniques, fluorescence signalling offers the advantages of high selectivity, sensitivity and rapid response.⁵ However, due to the poor coordination ability of aluminium, the development of its sensors is quite difficult as compared to other biologically important cations such as Cu(II), Pb(II), Hg(II), Zn(II) *etc.* Recently, a few fluorescence

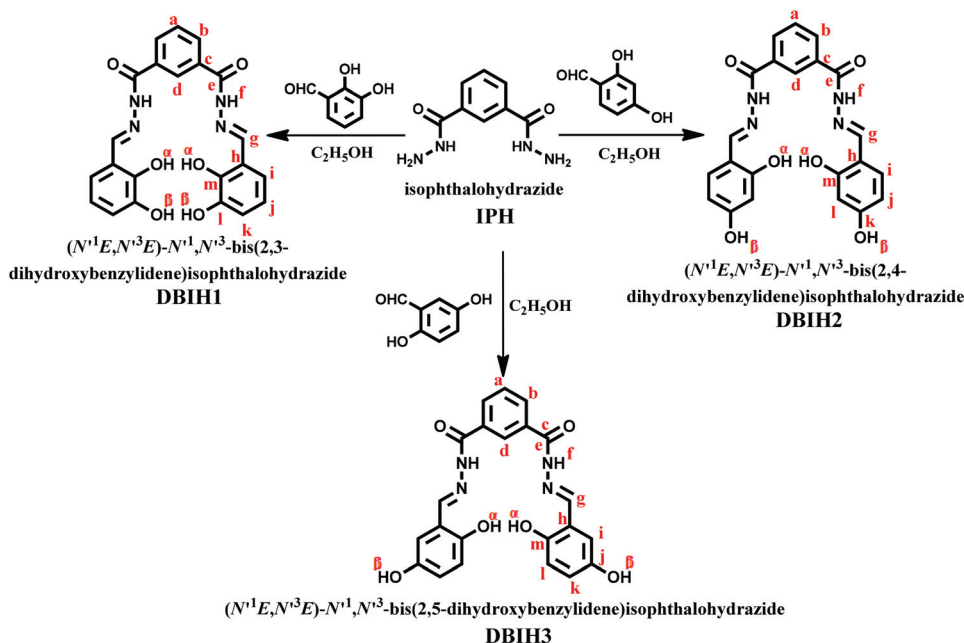
sensors for Al(III) have been reported based on various mechanisms such as photoinduced charge transfer (PET), intramolecular charge transfer (ICT), aggregation induced emission (AIE), excimer/excimer formation, fluorescence resonance energy transfer (FRET), C=N isomerization and chelation-enhanced fluorescence (CHEF).⁶ From the literature,⁶ it is clear that there are even fewer chemosensors which comply with all four desirable features in a chemical sensor at the same time, *i.e.* working in aqueous systems, low detection limit, high selectivity and applicability in living systems. We report here three probes which meet these criteria, namely they provide high selectivity with low detection limit in aqueous medium and have good response in biological systems.

Previously, our group reported sensors based on an aromatic platform which had imine, hydroxyl, urea/thiourea and thiosemicarbazides as receptor-cum-transducers for sensing.⁷ As an extension of our work on imine/hydroxyl containing probes, we have now designed systems **DBIH1–DBIH3** which contain a combination of –CONH, C=N and –OH groups (Scheme 1) to see their cooperative effect on sensing. Since Al(III) is a hard acid, accordingly it prefers systems containing hard base sites as O and N; hence, **DBIH1–DBIH3** provide an ideal co-ordination environment for selective and sensitive detection of Al(III) in HEPES buffer (pH 7.4, containing 30% DMSO as a co-solvent). Devoid of any conventional fluorophore, these easily synthesized systems provide a highly selective detection of Al(III) ions with high quantum yield. The detection limits achieved for **DBIH1–DBIH3** are 8.91, 14.1 and 19.95 nM comparable to the concentration range of Al(III) ions found in many chemical and biological systems. In addition, **DBIH1–DBIH3** have found practical application in the form of 'dip-sticks' which can provide instant detection of Al(III) and at

^aDepartment of Chemistry, UGC Center for Advance Studies, Guru Nanak Dev University, Amritsar 143005, Punjab, India. E-mail: geetahundal@yahoo.com

^bDepartment of Human Genetics, Guru Nanak Dev University, Amritsar 143005, Punjab, India

† Electronic supplementary information (ESI) available: Spectral characterization of sensors, UV spectral studies, fluorescence titration, Benesi–Hildebrand plots, Job's plots, detection limit and free energy calculations, competitive selectivity, spectral characterization and comparison of sensors with the literature and the MTT assay of chemosensors **DBIH1**, **DBIH2** and **DBIH3**. CCDC 995844. For ESI and crystallographic data in CIF or other electronic format see DOI: 10.1039/c4ob00329b



Scheme 1 Synthesis of sensors.

the same time in the estimation of Al(III) in live HeLa cells and C6 glioma cells using a confocal microscope.

Results and discussion

DBIH1–DBIH3 were synthesized by Schiff base condensation reaction (Scheme 1) and characterized by various spectroscopic techniques (Fig. S3 and S14[†]) and X-ray analysis (for **DBIH1**).

X-ray crystal structure of **DBIH1**

The two arms of the **DBIH1** are twisted with respect to each other and the central phenyl anchor, making dihedral angles of 16.9(1) and 31.4(1)° with the anchor, respectively, and 46.5(1)° between each other and they lie on opposite sides of the central phenyl ring (inset, Fig. 1). There is strong intramole-

cular H-bonding (Fig. 1) between the imine nitrogens N2 and N4 and the *ortho*-hydroxyl groups (O2–H2A···N2 2.678(4) and O5–H5A···N4 2.717(4) Å), respectively. The *meta*-hydroxyl group O3 at one end of the dipodal molecule is engaged in four intermolecular H-bonding interactions. It accepts one bond from the imine nitrogen N3 and hydroxyl oxygen O5 whereas it donates two H-bonds to imine N4 and carbonyl O4. The latter three H-bonds help in forming a zigzag chain parallel to the *b*-axis in a head to tail manner. The O6···O1 intermolecular H-bonding interactions between the hydroxyl group and the carbonyl oxygen (Table S2[†]) on the other end help in the formation of another zigzag chain parallel to the previous one (Fig. S1[†]), thus forming H-bonded undulating tapes, growing the crystal structure in the *bc* plane. The N3···O3 interactions result in similar but centrosymmetric tapes and the overall crystal structure ends up as a double helical H-bonded structure as shown down the *b*-axis (Fig. S2[†]).

¹H NMR of **DBIH1–DBIH3**

The chemical shifts of two –OH groups in the three isomers follow a trend since using the same concentration (5 mM), the α and β protons appear more downfield shifted in the *meta* isomer **DBIH2** (Fig. 2) which may be attributed to the *-ortho*, *-para* directing effect of the –OH groups, which causes a shielding effect on the C atoms bearing them. The aromatic protons ‘i’ of *meta* isomer are also much downfield shifted than ‘j’ and ‘l’ as they are shielded due to the presence of partial negative charge on them, owing to the +R effect of –OH groups.

Colorimetric and chromogenic spectral response of sensors (**DBIH1–DBIH3**)

The absorption spectrum of **DBIH1** exhibits a maximum centered at 318 nm ($\epsilon = 3.90 \times 10^4 \text{ M}^{-1} \text{ cm}^{-1}$) while for **DBIH2** at

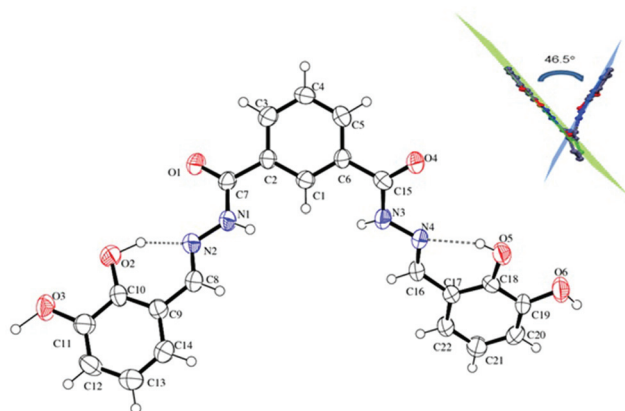


Fig. 1 ORTEP diagram of the **DBIH1** at 50% probability showing the labeling scheme. Inset: dihedral angle between two arms of **DBIH1**.

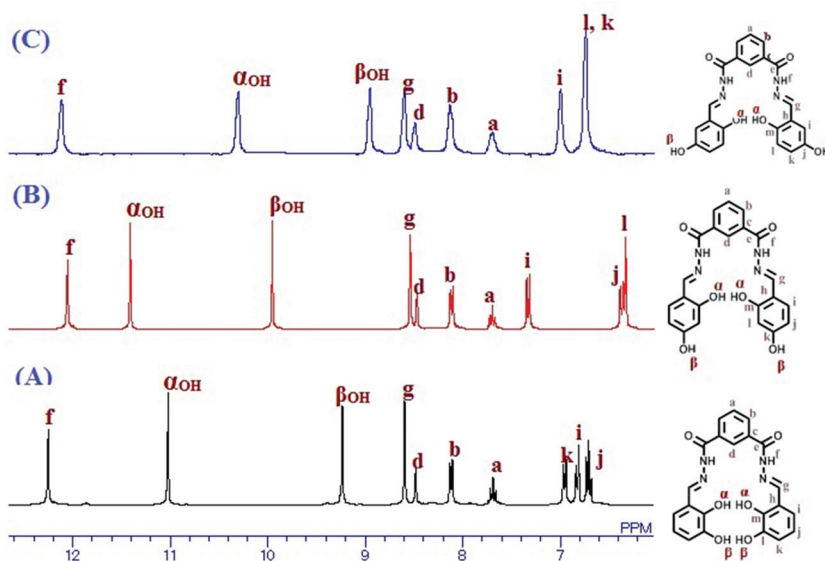


Fig. 2 ^1H NMR of (A) DBIH1, (B) DBIH2 and (C) DBIH3 at 5 mM concentration of each sensor.

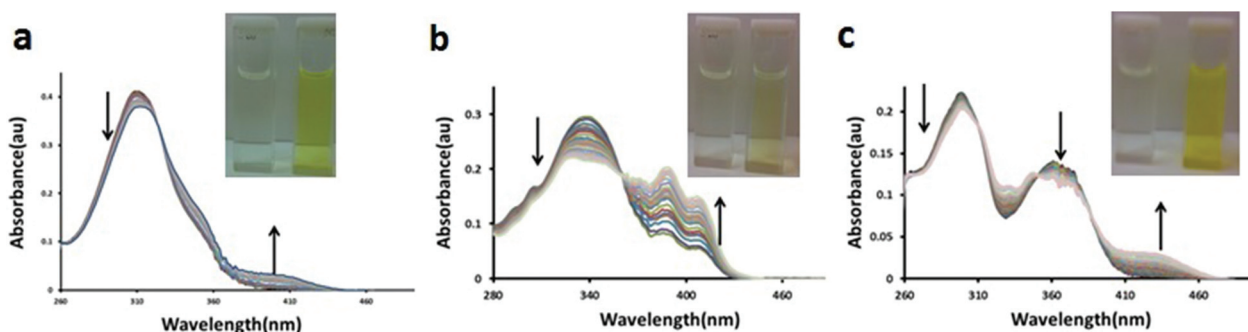


Fig. 3 Changes in absorption spectra of (a) DBIH1, (b) DBIH2 and (c) DBIH3 (10 μM) upon gradual addition of $\text{Al}(\text{III})$. Inset: color changes in sensor solutions with $\text{Al}(\text{III})$.

340 nm ($\epsilon = 3.09 \times 10^4 \text{ M}^{-1} \text{ cm}^{-1}$) in HEPES buffer (pH 7.4, containing 30% DMSO as a co-solvent). For **DBIH3**, the absorption spectrum exhibit bands centered at 296 nm ($\epsilon = 2.19 \times 10^4 \text{ M}^{-1} \text{ cm}^{-1}$) and at 358 nm ($\epsilon = 1.37 \times 10^4 \text{ M}^{-1} \text{ cm}^{-1}$) (Fig. S15–S17 \dagger). The absorption bands, ranging from 318 to 358 nm for the three sensors, have been designated as internal charge transfer (ICT) bands involving imine and hydroxyl groups.⁸

With $\text{Al}(\text{III})$, new bands are formed at λ_{max} 403 nm for **DBIH1**, at 384 and 403 for **DBIH2** and at 430 nm for **DBIH3**, with isobestic points at 328 nm, 358 nm and at 310, 351 and 387 nm, respectively (Fig. 3). These bathochromic shifts in all three cases are consistent with a color change from colorless to bright yellow (inset, Fig. 3). The presence of these isobestic points confirms the establishment of equilibrium between two species and reflects the formation of 1 : 1 complexes.

Fluorogenic spectral response of sensors (DBIH1–DBIH3)

Fluorescence characteristics of **DBIH1–DBIH3** (2.5 μM) were investigated in HEPES buffer (pH 7.4, containing 30% DMSO as a co-solvent). **DBIH1** and **DBIH3** exhibit very weak fluo-

rescence at λ_{em} 508 nm and λ_{em} 528 nm (excitation at 325 nm and 358 nm, respectively). Such a fluorescence is known to be due to the well-known ESIPT phenomenon in the case of Schiff bases.⁹ Whereas **DBIH2** shows a much weaker emission band at λ_{em} 455 nm (excitation at 340 nm) which may be due to the PET phenomenon owing to the availability of lone pairs of N of the $-\text{C}=\text{N}$ group and O of the OH group.¹⁰ This difference in their emission behaviour may again be attributed to the *ortho-para* directing capability of the $-\text{OH}$ groups which places partial negative charges on the $-\text{OH}$ bearing carbons in the case of *ortho* and *para* isomers, making them more susceptible to quinone forms, facilitating the proton transfer. These effects are corroborated by the observed chemical shift values of α - and β -OH and the aromatic protons (*vide supra*). All three isomers form a rigid chelated system with $\text{Al}(\text{III})$ due to coordination through OH and imine ($\text{CH}=\text{N}$) groups and consequently exhibit a strong fluorescence enhancement due to the CHEF mechanism.

DBIH1 exhibits strong fluorescence enhancement ($\Phi = 0.63$) upon addition of $\text{Al}(\text{III})$ centered at 508 nm (λ_{ex} 325 nm)

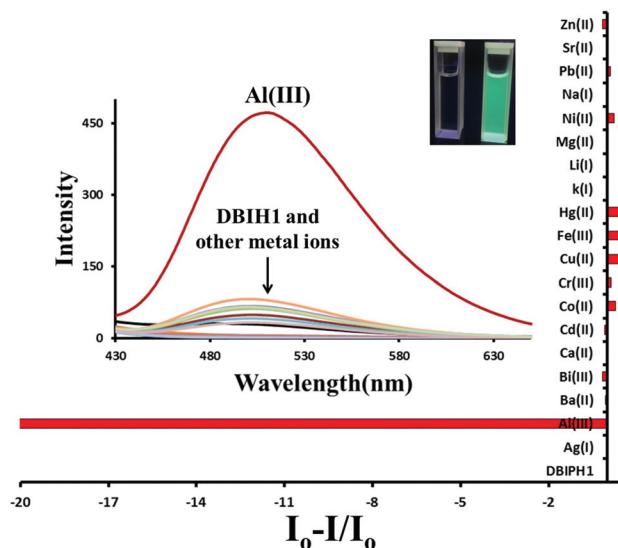


Fig. 4 Changes in fluorescence spectra of DBIH1 (2.5 μM) upon the addition of 10 equiv. of metal nitrates. Inset: color changes in sensor solution with Al(III) under a UV lamp.

(Fig. 4) accompanied by a green fluorescence (inset, Fig. 4). Similarly, upon Al(III) addition to DBIH2 a remarkable fluorescence enhancement (Fig. 5a) at λ_{em} 455 nm (λ_{ex} 340 nm) was observed with quantum yield¹¹ ($\Phi = 0.7$) giving blue fluorescence (inset, Fig. 5a). In DBIH3, when excited at λ_{ex} 358 nm after Al(III) addition, fluorescence enhancement (Fig. 5b) was observed at 528 nm with quantum yield ($\Phi = 0.77$) yielding green fluorescence (inset, Fig. 5b). For all the sensors, the addition of Li(I), Na(I), K(I), Ag(I), Mg(II), Ca(II), Cd(II), Ba(II), and Sr(II) showed no significant change, whereas Bi(III) and Zn(II) caused very little enhancement and Co(II), Cr(III), Cu(II), Ni(II), Hg(II), Pb(II), and Fe(III) showed quenching to different extents.^{10d,12} Selectivity of sensors DBIH1–DBIH3 showed no change when other aluminium salts such as $\text{Al}_2(\text{SO}_4)_3$ and

AlCl_3 were used (Fig. S30, S32 and S34[†]). Consequently, due to significant response of sensors towards Al(III), all the further studies were carried out with Al(III) only.

Job's plot¹³ obtained from emission data showed 1:1 stoichiometry for all the Al(III) complexes of DBIH1–DBIH3 (Fig. S21–S23[†]). This complex formation was further supported by ESI/MS, peaks at m/z 459.0798 $[(\text{M} - 2\text{H}) + \text{Al}(\text{III})]^+$ (calc. 459.0885), 495.0797 $[(\text{M} - 2\text{H}) + \text{Al}(\text{III}) + 2\text{H}_2\text{O}]^+$ (calc. 495.1097), 537.0963 $[(\text{M} - 2\text{H}) + \text{Al}(\text{III}) + \text{NO}_3^- + \text{H}_2\text{O} - 2]^+$ (calc. 537.0713), 615.1080 $[(\text{M} - 2\text{H}) + \text{Al}(\text{III}) + \text{NO}_3^- + \text{H}_2\text{O} + \text{DMSO} - 2]^+$ (calc. 615.0852) for DBIH1. Similarly, peaks at m/z 459.0888, 537.1035, 615.1165 for DBIH2 and at m/z 459.0457, 537.1008, 615.0988 for DBIH3 were observed (Fig. S37, S39 and S41[†]). The occurrence of a peak at 537.07 in all three cases indicates the formation of the proposed $[(\text{C}_{22}\text{H}_{18}\text{AlN}_5\text{O}_{10}) - 2]$ complex (Fig. 6).

Titration of DBIH1–DBIH3 with Al(III) (Fig. S24, S26 and S28[†]) was followed by fluorescence to determine binding constants, $5.57 \times 10^5 \text{ M}^{-1}$, $2.5 \times 10^6 \text{ M}^{-1}$ and $7.0 \times 10^4 \text{ M}^{-1}$, respectively, employing the Benesi–Hildebrand plot¹⁴ (Fig. S25(a), S27(a) and S29(a)[†]) [comparable to the absorbance data (Fig. S18, S19 and S20[†])]. The metal complexation is confirmed by the free energy values of the complexation processes such as $-32.75 \text{ kJ mol}^{-1}$, $-36.50 \text{ kJ mol}^{-1}$ and $-27.64 \text{ kJ mol}^{-1}$ for DBIH1–DBIH3, respectively, obtained using the equation $\Delta G = -2.303 RT \log K_a$ (S20). Respective detection limits of these sensors for Al(III) calculated according to the literature¹⁵ were found to be $8.91 \times 10^{-9} \text{ M}$, $14.1 \times 10^{-9} \text{ M}$ and $19.95 \times 10^{-9} \text{ M}$, which are quite low to detect the submicromolar concentration of Al(III) (Fig. S25(b), S27(b) and S29(b)[†]).

Competitive selectivity of DBIH1–DBIH3 for Al(III) (Fig. S31, S33 and S35[†]) was determined by fluorescence titration with Al(III) in the presence of other metal ions under study, which revealed that Al(III) can be detected in the presence of other competitive metal ions. For this experiment, DBIH1–DBIH3 were treated with 10 equivalents of Al(III) in the presence of 50

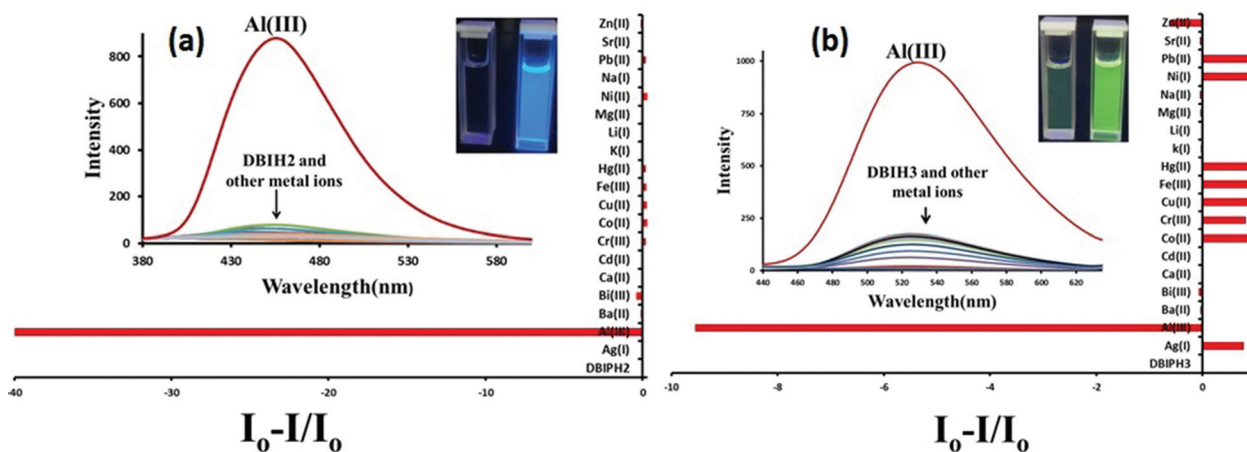


Fig. 5 Changes in fluorescence spectra of (a) DBIH2 and (b) DBIH3 (2.5 μM) upon the addition of 10 equiv. of metal nitrates under study. Inset: color changes in sensor solutions with Al(III) under a UV lamp.

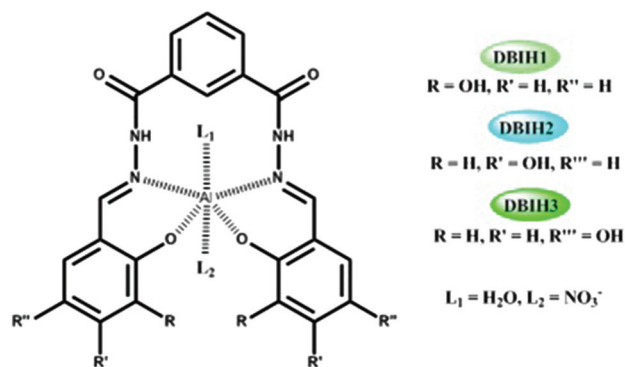


Fig. 6 Proposed structure of Al(III) complexes of DBIH1–DBIH3.

equivalents of other metal ions under study. There is no significant interference for the detection of Al(III) in the presence of other metal ions except in the case of Cu(II) and Fe(III) which showed some quenching of fluorescence but enhancement is still very prominent.

¹H NMR titration experiments of sensors (DBIH1–DBIH3)

In order to investigate the mode of the binding sensor to Al(III) ions, NMR titrations were carried out in DMSO-*d*₆ (Fig. 7). In all the cases, signals due to α -OH protons disappear as a result of deprotonation and complexation but those of β -OH, imine and –NH groups sustain. The chemical shift values of β -OH protons show low frequency shifts in DBIH1 and DBIH2 ($\Delta\delta$ 0.042 and 0.712) and a high frequency shift in DBIH3 ($\Delta\delta$ 0.267), which may be due to different kinds and extents of H-bonding interactions. The complexation was confirmed by isolating the solid complexes by reacting DBIH1–DBIH3 with

Al(NO₃)₃·9H₂O in ethanol and characterizing them using NMR, IR and mass spectroscopy (Fig. S36–S41†).

In order to check the practical applicability of DBIH1–DBIH3, we prepared dip sticks by coating paper strips with DMSO–H₂O solution of sensors. After drying, these strips were dipped in the solution (5 μ M) of Al(NO₃)₃ in distilled water, dried and observed under a UV lamp. Similar color changes were observed in the solid state (Fig. 8) as those found earlier in the solution state. The different fluorescent colors obtained not only detect the presence of Al(III) but also distinguish between three positional isomers.

Bioimaging of Al(III) in live cells

For the investigation of biological applications of the sensors DBIH1–DBIH3, cell imaging studies have been performed with both the human cervical cancer cell line (HeLa cells) (Fig. 9) and glial cells of the rat brain (C6 glioma cells) (Fig. 10). Both the HeLa and C6 glioma cells, themselves and after incubation with Al(III) (10 μ M and 50 μ M), did not exhibit any fluorescence (Fig. 9(a)–9(c) and 10(a)–10(c), respectively). Further, HeLa and C6 glioma cells were incubated with 10 μ M of DBIH1, DBIH2 and DBIH3 for 30 min at 37 °C. When imaged after incubation, HeLa as well as C6 glioma cells showed no fluorescence for DBIH1 (Fig. 9(d), 10(d)) and DBIH2 (Fig. 9(g), 10(g)) but faint green fluorescence for DBIH3 (Fig. 9(j) and 10(j)) was observed in both HeLa and C6 glioma cells. The excitation laser used for DBIH1, DBIH2 and DBIH3 was 405 nm. Once the treated cells (HeLa and C6 glioma) were incubated with Al(III) (10 μ M) for another 30 min at 37 °C, bright green fluorescence was observed in both the types of cells for DBIH1 (Fig. 9(e) and 10(e)) which increased significantly with 50 μ M Al(III) (Fig. 9(f) and 10(f)). Similarly, green

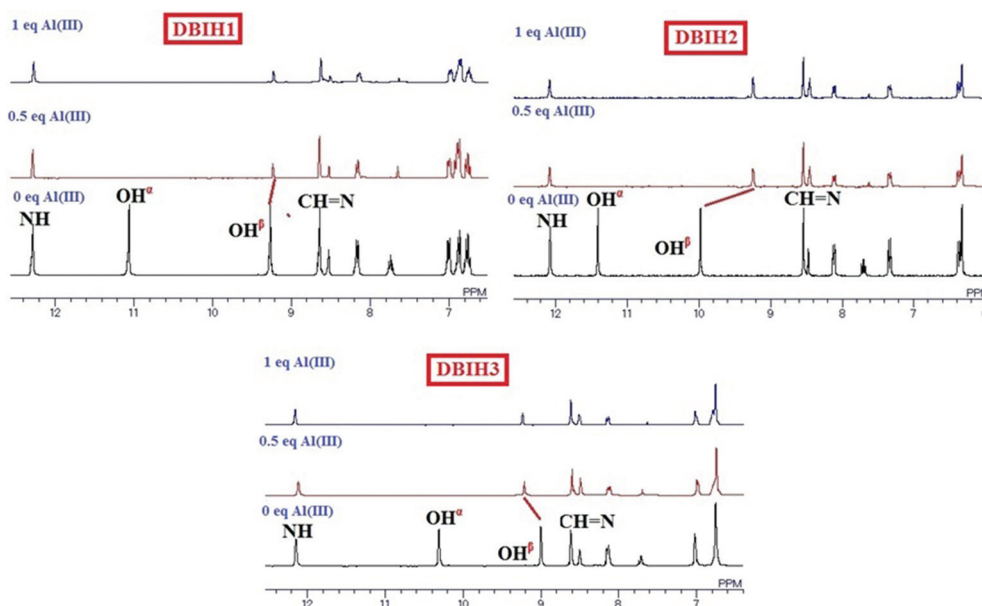


Fig. 7 Changes in partial ¹H NMR of DBIH1–DBIH3 (5 mM) upon the addition of Al(III) in DMSO-*d*₆.

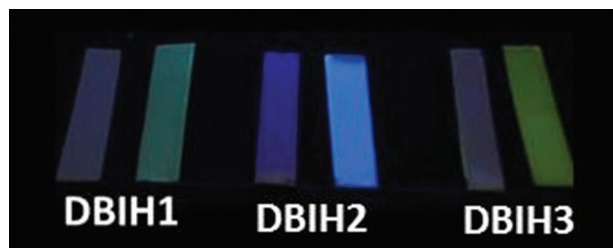


Fig. 8 Fluorescent color changes with dip sticks formed from DBIH1–DBIH3 (2.5 μM) in DMSO–H₂O upon treatment with 5 μM of Al(III). Left – before and right – after Al(III) treatment.

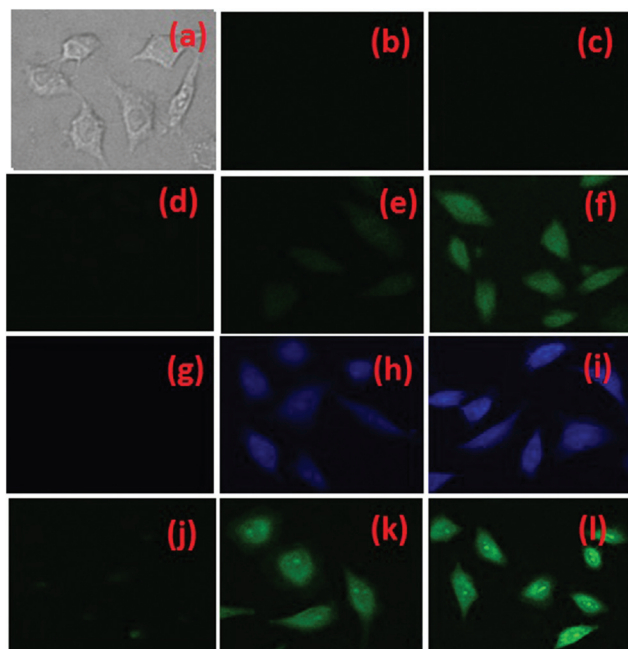


Fig. 9 Images of HeLa cells: (a) brightfield image of HeLa cells, (b) fluorescence image of HeLa cells incubated with Al(III) (10 μM) for 30 min, (c) fluorescence image of HeLa cells incubated with Al(III) (50 μM) for 30 min, (d) fluorescence image of HeLa cells incubated with DBIH1 (10 μM) for 30 min and further incubation with (e) 10 μM Al(III) and (f) 50 μM Al(III), (g) fluorescence image of HeLa cells incubated with DBIH2 (10 μM) for 30 min and further incubation with (h) 10 μM Al(III) and (i) 50 μM Al(III), (j) fluorescence image of HeLa cells incubated with DBIH3 (10 μM) for 30 min and further incubation with (k) 10 μM Al(III) and (l) 50 μM Al(III).

fluorescence of DBIH3 got enhanced when incubated with Al(III) (10 μM) (Fig. 9(k) and 10(k)) and fluorescence got further enhanced significantly with 50 μM Al(III) (Fig. 9(l) and 10(l)). For DBIH2, blue fluorescence was observed with 10 μM Al(III) treatment (Fig. 9(h) and 10(h)) which also increased considerably with 50 μM Al(III) (Fig. 9(i) and 10(i)) in both the tested cell lines. The fluorescence was observed in the perinuclear region as well as the cytosol; hence, it indicates that chemosensors DBIH1, DBIH2 and DBIH3 are permeable to HeLa and C6 glioma cells and can be used for detecting Al(III) in the live cells.

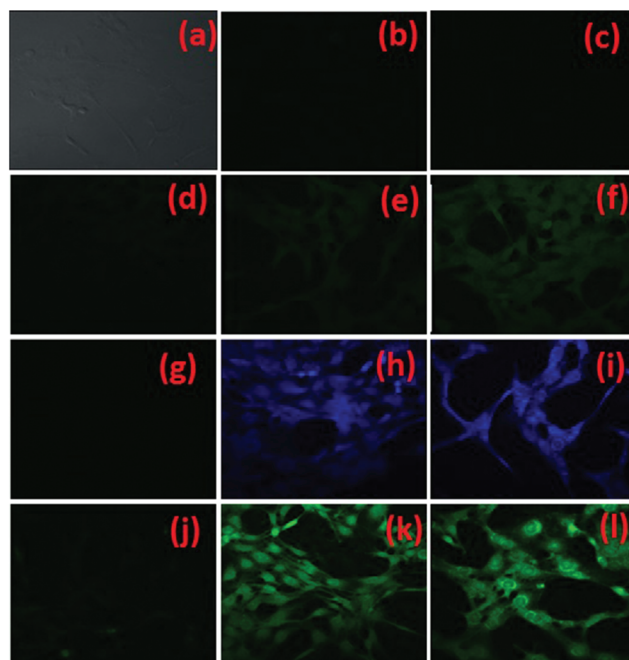


Fig. 10 Images of C6 glioma cells: (a) brightfield image of C6 glioma cells, (b) fluorescence image of C6 glioma cells incubated with Al(III) (10 μM) for 30 min, (c) fluorescence image of C6 glioma cells incubated with Al(III) (50 μM) for 30 min, (d) fluorescence image of C6 glioma cells incubated with DBIH1 (10 μM) for 30 min and further incubation with (e) 10 μM Al(III) and (f) 50 μM Al(III), (g) fluorescence image of C6 glioma cells incubated with DBIH2 (10 μM) for 30 min and further incubation with (h) 10 μM Al(III) and (i) 50 μM Al(III), (j) fluorescence image of C6 glioma cells incubated with DBIH3 (10 μM) for 30 min and further incubation with (k) 10 μM Al(III) and (l) 50 μM Al(III).

To investigate the cytotoxicity of DBIH1, DBIH2 and DBIH3, the MTT assay with HeLa cells as well as C6 glioma cells was performed. No significant differences in the proliferation of the HeLa and C6 glioma cells were observed in the absence or presence of 10 μM of chemosensors DBIH1 and DBIH3 (80–90% cell viability with the chemosensor DBIH1 and 90–94% cell viability with DBIH3) for both the tested cell lines (Fig. S42[†]). However, with the chemosensor DBIH2 HeLa cells showed nearly 27% cell survival while C6 glioma cells had more than 50% (53%) cell viability, indicating the chemosensor DBIH2 to be toxic for the cells. With Al(III) (50 μM) alone there was not much effect on cell viability (90% cell viability) with both the tested cell lines. Again, addition of 10 μM or 50 μM of Al(III) in the presence of chemosensors DBIH1 and DBIH3 (10 μM) did not show any significant effect but DBIH2 showed a considerable effect on the cell viability of both the cell types. These data show that chemosensors DBIH1 and DBIH3 have very low cytotoxicity while DBIH2 is substantially cytotoxic.

In conclusion, we have reported a series of three chromo-fluorogenic sensors for Al(III) which can detect Al(III) up to the nanomolar level, with high quantum yields in aqueous medium. The detection mechanism involved is CHEF activation due to the formation of rigid aluminium complexes.

Additionally, on complexation these positional isomers can be distinguished visually under UV light illumination, as well as by dip stick experiment, even at 5 μM of $\text{Al}(\text{III})$ without the aid of any sophisticated instrument. Moreover, cell imaging experiments with HeLa cells and C6 glioma cells establish the utility of these sensors for tracking $\text{Al}(\text{III})$ in live cells.

Experimental

General procedures

All the commercially available chemicals were purchased from Aldrich and used without further purification. All solvents were dried by standard methods. Dimethyl isophthalate (DIP) and isophthalohydrazide (IPH) were prepared according to literature methods.¹⁶ TLC was carried out on glass sheets pre-coated with silica gel. Elemental analyses (C, H, N) were performed on a Perkin-Elmer model 2400 CHN analyzer. The ^1H and ^{13}C NMR spectra were carried out in DMSO-d_6 with TMS as an internal reference on a JEOL-FT NMR-300 MHz spectrophotometer. The infrared spectra (KBr pellet) were recorded using a Perkin-Elmer FT-IR C92035 spectrophotometer in the range 400–4000 cm^{-1} . The electronic absorption spectra were recorded on a Shimadzu Pharmaspec UV-1700 UV-vis spectrophotometer with a quartz cuvette (path length, 1 cm). The absorption spectra have been recorded between 1100 and 200 nm. The cell holder of the spectrophotometer was thermostated at 25 $^\circ\text{C}$ for consistency in the recordings. Fluorescence spectra were recorded on a Varian fluorospectrophotometer. HRMS spectra were recorded on a Bruker's microTOF-QII spectrophotometer.

X-Ray measurements and structure determination

The crystals of the compound **DBIH1** were grown by slow evaporation from a mixture of *N,N*-dimethylformamide and ethanol. X-Ray data were collected on a Bruker's Apex-II CCD diffractometer using $\text{Mo K}\alpha$ ($\lambda = 0.71069 \text{ \AA}$) at room temperature. The data were corrected for Lorentz and polarization effects and empirical absorption corrections were applied using SADABS from Bruker. A total of 15 046 reflections were measured out of which 3788 were independent and 1850 were observed [$I > 2\sigma(I)$] for theta 26 $^\circ$. The structures were solved by direct methods using SIR-92 and refined by full-matrix least squares refinement methods based on F^2 using SHELX-97. The hydrogens of the –OH and –NH groups were located from the difference Fourier synthesis and were refined isotropically with U_{iso} values 1.2 times that of their carrier oxygen atoms, with restraints on the bond distances. All non-hydrogen atoms were refined anisotropically. All other hydrogen atoms were fixed geometrically with their U_{iso} values 1.2 times those of the phenylene carbons. All calculations were performed using the Wingx [3] package. The important crystal and refinement parameters are given in Table S1.†

UV-vis and fluorescence studies

Molecular interactions of **DBIH1**, **DBIH2** and **DBIH3** with 19 different metal nitrates under study were investigated by UV-vis spectroscopy at 10^{-5} M and fluorescence spectroscopy at 2.5×10^{-6} M in HEPES buffer (pH 7.4, containing 30% DMSO as a co-solvent). Stock solutions of **DBIH1**, **DBIH2** and **DBIH3** (10^{-3} M) and of metal nitrates (10^{-1} – 10^{-3} M) were prepared in DMSO and distilled water respectively. Selectivity tests were performed by 2.5×10^{-6} M of all the sensors and 10 equiv. of $\text{Al}(\text{III})$ in the presence of 50 equiv. of other interfering metal ions. The binding stoichiometries of $\text{Al}(\text{III})$ complexes of **DBIH1**–**DBIH3** were determined by the method of continuous variation (Job's plot). Ten solutions were prepared by varying the *L/M* ratio and keeping the total concentration of all the sensors and the cationic guest constant (2.5×10^{-5} M) with continuous variation of mole fraction of **DBIH1**–**DBIH3**. The results indicate the formation of complexes with a stoichiometric ratio of 1:1. The stability constant was determined using a Benesi–Hildebrand plot in each case.

Calculation of quantum yield

The fluorescence quantum yield Φ_f for **DBIH1**–**DBIH3** was determined at room temperature using optically matching solutions of 9,10-diphenylanthracene ($\Phi_f = 0.90$) in ethanol as the standard at an excitation wavelength of 325, 340 and 358 nm respectively. The quantum yield was calculated using eqn (1), in which Φ_{fs} is the radiative quantum yield of the sample, Φ_{fr} is the radiative quantum yield of the reference, A_s and A_r are the absorbances of the sample and the reference, respectively, D_s

$$\Phi_{\text{fs}} = \Phi_{\text{fr}} \times \frac{1 - 10^{-A_s L_s}}{1 - 10^{-A_r L_r}} \times \frac{N_s^2}{N_r^2} \times \frac{D_s}{D_r} \quad (1)$$

and D_r are the areas of emission for the sample and the reference, L_s and L_r are the lengths of the absorption cells, and N_s and N_r are the refractive indices of the sample and reference solutions (pure solvents were assumed).

Cell imaging studies

Both the tested cell lines (HeLa and C6 glioma) were grown in Dulbecco's modified Eagle's medium (DMEM) supplemented with 10% fetal bovine serum (FBS) and 100 IU ml^{-1} penicillin, 100 $\mu\text{g ml}^{-1}$ streptomycin and 100 $\mu\text{g ml}^{-1}$ gentamycin. The cells were maintained in a humidified incubator at 37 $^\circ\text{C}$ with 5% CO_2 . On the day before treatment, a total of 2×10^5 cells were seeded on 11 mm glass coverslips into each well of a 24-well plate and these were grown for 24 hours (till 60–70% confluence) and treatment was carried out in triplicates in FBS and antibiotic free media. HeLa and C6 glioma cells were incubated with three different ligands, *i.e.*, **DBIH1**, **DBIH2** and **DBIH3** (10 μM) (each in triplicates), at 37 $^\circ\text{C}$ with 5% CO_2 for 30 min followed by three times washing with 1 \times phosphate buffered saline (PBS) (pH = 7.4) and treatment with $\text{Al}(\text{III})$ (10 μM and 50 μM conc. each in three replicates) for another 30 min by incubating the cells under the same conditions. The

cells were then washed three times with $1 \times$ PBS, fixed in ice cold 4% paraformaldehyde, washed again three times with $1 \times$ PBS and mounted on glass slides. To investigate the cytotoxicity of **DBIH1**, **DBIH2** and **DBIH3**, the MTT [3-(4,5-dimethylthiazol-2-yl)-2,5-diphenyltetrazolium bromide] assay with HeLa cell lines as well as C6 glioma cells was performed to determine the effect of **DBIH1**, **DBIH2** and **DBIH3** on cell proliferation. Confocal microscopy imaging was performed on a NIKON A1R confocal laser scanning microscope using diode laser excitation at 405 nm. Imaging was performed using Plan Apo 60 \times oil immersion objective lens.

Synthesis of compounds

Synthesis of DBIH1. 200 mg (1.02 mmol) of IPH was dissolved in 10 ml of ethanol to which was added 284 mg (2.05 mmol) of 2,3-dihydroxybenzaldehyde in 10 ml of ethanol along with 2–3 mg of zinc perchlorate. The color of the solution changed immediately to turbid yellow and precipitates were separated out within 10 minutes. These precipitates were filtered, washed with methanol and dried under vacuum for 24 hours. Yield 90%. Light yellow solid. Mp = 238–240 $^{\circ}$ C; 1 H NMR (300 MHz, DMSO- d_6) (Fig. S1, ESI † δ): 6.78 (t, 2H, Ar, J = 7.8 Hz), 6.89 (d, 2H, Ar, J = 6.6 Hz), 7.03 (d, 2H, Ar, J = 6.6 Hz), 7.76 (t, 1H, Ar, J = 7.5 Hz), 8.19 (d, 2H, Ar, J = 7.8 Hz), 8.56 (s, 1H, Ar), 8.67 (s, 2H, -CH=N), 9.31 (s, 2H, -OH); 13 C NMR (75 MHz, DMSO- d_6) (Fig. S2, \dagger δ): 117.8 (Ar), 119.2 (Ar), 119.6 (Ar), 120.3 (Ar), 127.4 (Ar), 129.4 (Ar), 131.4 (Ar), 133.6 (Ar), 146.0 (CH=N), 146.5 (-C-OH), 149.6 (-C-OH), 162.6 (-C=O); FTIR (KBr, cm^{-1}) (Fig. S3 †): 3299 (OH), 3090 (NH), 1647 (C=O), 1609 (C=N); elemental analysis calculated for $\text{C}_{22}\text{H}_{18}\text{N}_4\text{O}_6$: C, 60.83; H, 4.18; N, 12.90%. Found: C, 61.34; H, 4.20; N, 11.32%; HRMS m/z (Fig. S4 †): 457.1046 $[\text{M} + \text{Na}]^+$ ion (calc. 457.1119).

Synthesis of DBIH2. The same procedure as that for **DBIH1** was used except that 2,4-dihydroxybenzaldehyde was used in place of 2,3-dihydroxybenzaldehyde. The color of the solution changed immediately to light orange and precipitates were separated out within half an hour. These precipitates were filtered, washed with chilled methanol and dried under vacuum for 24 hours. Yield 80%. Orange solid. Mp = 298–300 $^{\circ}$ C; 1 H NMR (300 MHz, DMSO- d_6) (Fig. S5, \dagger δ): 6.33 (s, 2H, Ar), 6.36 (d, 2H, Ar, J = 8.4 Hz), 7.33 (d, 2H, Ar, J = 8.1 Hz), 7.69 (t, 1H, Ar, J = 8.1 Hz), 8.12 (d, 2H, Ar, J = 7.8 Hz), 8.47 (s, 1H, Ar), 8.54 (s, 2H, -CH=N), 9.95 (s, 2H, -OH), 11.40 (s, 2H, -OH), 12.05 (s, 2H, -NH); 13 C NMR (75 MHz, DMSO- d_6) (Fig. S6, \dagger δ): 102.6 (Ar), 107.7 (Ar), 110.5 (Ar), 126.7 (Ar), 128.8 (Ar), 130.6 (Ar), 131.3 (Ar), 133.3 (Ar), 149.5 (CH=N), 159.4 (-C-OH), 160.8 (-C-OH), 161.9 (-C=O); FTIR (KBr, cm^{-1}) (Fig. S7 †): 3349 (OH), 3128 (NH), 1660 (C=O), 1607 (C=N); elemental analysis calculated for $\text{C}_{22}\text{H}_{18}\text{N}_4\text{O}_6$: C, 60.83; H, 4.18; N, 12.90%. Found: C, 60.86; H, 4.16; N, 12.87%; HRMS m/z (Fig. S8 †): 435.1283 $[\text{M} + 1]^+$ (calc. 435.1299).

Synthesis of DBIH3. In this case 2,5-dihydroxybenzaldehyde was used in place of 2,3-dihydroxybenzaldehyde. The color of the solution changed immediately to brownish orange and precipitates were separated out within an hour. These precipitates

were filtered, washed with chilled methanol and dried. Yield 50%. Yellow solid. Mp = 300–302 $^{\circ}$ C; 1 H NMR (300 MHz, DMSO- d_6) (Fig. S9, \dagger δ): 6.75 (4H, s, Ar), 7.01 (2H, s, Ar), 7.71 (1H, t, Ar, J = 7.8 Hz), 8.13 (2H, d, Ar, J = 8.1 Hz), 8.50 (1H, s, Ar), 8.61 (2H, s, -CH=N), 8.96 (2H, s, -OH), 10.31 (2H, s, -OH), 12.13 (2H, s, -NH); 13 C NMR (75 MHz, DMSO- d_6) (Fig. S10, \dagger δ): 113.6 (Ar), 117.2 (Ar), 119.1 (Ar), 127.0 (Ar), 128.9 (Ar), 130.9 (Ar), 133.4 (Ar), 147.8 (CH=N), 149.9 (-C-OH), 150.3 (-C-OH), 162.3 (-C=O); IR (KBr, cm^{-1}) (Fig. S11 †): 3385 (OH), 3204 (NH), 1625 (C=O), 1580 (C=N); elemental analysis calculated for $\text{C}_{22}\text{H}_{18}\text{N}_4\text{O}_6$: C, 60.83; H, 4.18; N, 12.90%. Found: C, 60.38; H, 4.19; N, 12.11%; HRMS m/z (Fig. S12 †): 435.1300 $[\text{M} + 1]^+$ (calc. 435.1299).

Synthesis of the DBIH1-Al(III) complex. To a 5 ml suspension of **DBIH1** (0.05 g, 1.15 mmol) in ethanol, a 10 ml solution of $\text{Al}(\text{NO}_3)_3 \cdot 9\text{H}_2\text{O}$ (0.086 g, 2.30 mmol) in distilled water was added dropwise over 15 minutes and then stirred for half an hour. After stirring, the reaction mixture was concentrated and placed in an ice bath. The dark brown precipitates were collected on a Buchner funnel. Mp = 300–302 $^{\circ}$ C. 1 H NMR (300 MHz, DMSO- d_6) (Fig. S28(a), \dagger δ): 6.74 (t, 2H, Ar, J = 7.5 Hz), 6.86 (d, 2H, Ar, J = 7.5 Hz), 6.98 (d, 2H, Ar, J = 7.8 Hz), 7.72 (t, 1H, Ar, J = 7.5 Hz), 8.14 (d, 2H, Ar, J = 7.8 Hz), 8.51 (s, 1H, Ar), 8.63 (s, 2H, -CH=N), 9.27 (s, 2H, -OH), 12.30 (s, 2H, -NH); IR (KBr, cm^{-1}) (Fig. S28(b) †): 3242 (OH), 3064 (NH), 1660 (C=O), 1614 (C=N), 1385 (-NO $_3$); HRMS m/z (Fig. S29 †): 459.0798 $[(\text{M} - 2\text{H}) + \text{Al}(\text{III})]^+$ (calc. 459.0885), 495.0797 $[(\text{M} - 2\text{H}) + \text{Al}(\text{III}) + 2\text{H}_2\text{O}]^+$ (calc. 495.1097), 537.0963 $[(\text{M} - 2\text{H}) + \text{Al}(\text{III}) + \text{NO}_3^- + \text{H}_2\text{O} - 2]^+$ (calc. 537.0713), 615.1080 $[(\text{M} - 2\text{H}) + \text{Al}(\text{III}) + \text{NO}_3^- + \text{H}_2\text{O} + \text{DMSO} - 2]^+$ (calc. 615.0852).

Synthesis of the DBIH2-Al(III) complex. To a 5 ml solution of **DBIH2** (0.05 g, 1.15 mmol) in ethanol, a 10 ml solution of $\text{Al}(\text{NO}_3)_3 \cdot 9\text{H}_2\text{O}$ (0.086 g, 2.30 mmol) in distilled water was added dropwise over 15 minutes and then stirred for half an hour. After stirring, the reaction mixture was concentrated and placed in an ice bath. The dark brown precipitates were collected on a Buchner funnel. Mp = 300–302 $^{\circ}$ C; 1 H NMR (300 MHz, DMSO- d_6) (Fig. S30(a), \dagger δ): 6.33 (s, 2H, Ar), 6.35 (d, 2H, Ar, J = 8.4 Hz), 7.33 (d, 2H, Ar, J = 8.9 Hz), 7.69 (t, 1H, Ar, J = 8.1 Hz), 8.10 (d, 2H, Ar, J = 8.1 Hz), 8.45 (s, 1H, Ar), 8.54 (s, 2H, -CH=N), 9.91 (s, 2H, -OH), 12.05 (s, 2H, -NH); IR (KBr, cm^{-1}) (Fig. S30(b) †): 3391 (OH), 3206 (NH), 1639 (C=O), 1618 (C=N), 1385 (-NO $_3$); HRMS m/z (Fig. S31 †): 459.0888 $[(\text{M} - 2\text{H}) + \text{Al}(\text{III})]^+$ (calc. 459.0885), 537.1035 $[(\text{M} - 2\text{H}) + \text{Al}(\text{III}) + \text{NO}_3^- + \text{H}_2\text{O} - 2]^+$ (calc. 537.0713), 615.1165 $[(\text{M} - 2\text{H}) + \text{Al}(\text{III}) + \text{NO}_3^- + \text{H}_2\text{O} + \text{DMSO} - 2]^+$ (calc. 615.0852).

Synthesis of the DBIH3-Al(III) complex. To a 5 ml solution of **DBIH3** (0.05 g, 1.15 mmol) in ethanol, a 10 ml solution of $\text{Al}(\text{NO}_3)_3 \cdot 9\text{H}_2\text{O}$ (0.086 g, 2.30 mmol) in distilled water was added dropwise over 15 minutes and then stirred for half an hour. After stirring, the reaction mixture was concentrated and placed in an ice bath. The dark brown precipitates were collected on a Buchner funnel. Mp = 300–302 $^{\circ}$ C; 1 H NMR (300 MHz, DMSO- d_6) (Fig. S32(a), \dagger δ): 6.75 (s, 4H, Ar); 7.00 (s, 2H, Ar); 7.71 (t, 1H, Ar, J = 7.8 Hz); 8.13 (d, 2H, Ar, J = 8.1 Hz); 8.49 (s, 1H, Ar); 8.61 (s, 2H, -CH=N); 10.17 (s, 2H, -OH); 12.13

(s, 2H, -NH); IR (KBr, cm^{-1}) (Fig. S32(b)†): 3408 (OH), 3250 (NH), 1666 (C=O), 1590 (C=N), 1385 ($-\text{NO}_3$); HRMS m/z (Fig. S33†): HRMS m/z : 459.0457 $[(\text{M} - 2\text{H}) + \text{Al}(\text{III})]^+$ (calc. 459.0885), 537.1008 $[(\text{M} - 2\text{H}) + \text{Al}(\text{III}) + \text{NO}_3^- + \text{H}_2\text{O} - 2]^+$ (calc. 537.0713), 615.0988 $[(\text{M} - 2\text{H}) + \text{Al}(\text{III}) + \text{NO}_3^- + \text{H}_2\text{O} + \text{DMSO} - 2]^+$ (calc. 615.0852).

Acknowledgements

MSH and GH are thankful to CSIR (India) for research grant no. 01(2406)/10/EMR-II. SS is thankful to UGC for a senior research fellowship. Live cell imaging was supported by DBT, India (BT/IN/German/13/VK/2010) and BMBF (IND 10/036) to VV under the framework of the Indo-German bilateral cooperation for research.

References

- (a) G. Berthon, *Coord. Chem. Rev.*, 2002, **228**, 319; (b) F. Aguilar, H. Autrup, S. Barlow, L. Castle, R. Crebelli, W. Dekant, K.-H. Engel, N. Gontard, D. Gott, S. Grilli, R. Gürtler, J.-C. Larsen, C. Leclercq, J.-C. Leblanc, F.-X. Malcata, W. Mennes, M.-R. Milana, I. Pratt, I. Rietjens, P. Tobback and F. Toldrá, *EFSA J.*, 2008, **754**, 1; (c) M. I. Yousef, A. M. El-Morsy and M. S. Hassan, *Toxicology*, 2005, **215**, 97; (d) J. L. Greger and J. E. Sutherland, *Crit. Rev. Clin. Lab. Sci.*, 1997, **34**, 439; (e) E. DeVoto and R. A. Yokel, *Environ. Health Perspect.*, 1994, **102**, 940.
- (a) G. D. Fasman, *Coord. Chem. Rev.*, 1996, **149**, 125; (b) T. P. Flaten, *Brain Res. Bull.*, 2001, **55**, 187; (c) M. Baral, S. K. Sahoo and B. K. Kanungo, *J. Inorg. Biochem.*, 2008, **102**, 1581; (d) C. Exley, A. Begum, M. P. Woolley and R. N. Bloor, *Am. J. Med.*, 2006, **119**, 276.
- (a) D. L. Godbold, E. Fritz and A. Hüttermann, *Proc. Natl. Acad. Sci. U.S.A.*, 1988, **85**, 3888; (b) E. Delhaize and P. R. Ryan, *Plant Physiol.*, 1995, **107**, 315.
- (a) J. Barcaló and C. Poschenrieder, *Environ. Exp. Bot.*, 2002, **48**, 75; (b) B. Valeur and I. Leray, *Coord. Chem. Rev.*, 2000, **205**, 3; (c) Z. Krejpcio and R. W. Wójcziak, *Environ. Stud.*, 2002, **11**, 251.
- (a) A. T. Wright and E. V. Anslyn, *Chem. Soc. Rev.*, 2006, **35**, 14; (b) L. Prodi, *New J. Chem.*, 2005, **29**, 20; (c) J. Yoon, S. K. Kim, N. J. Singh and K. S. Kim, *Chem. Soc. Rev.*, 2006, **35**, 355; (d) V. Amendola and L. Fabbrizzi, *Chem. Commun.*, 2009, 513; (e) R. W. Sinkeldam, N. J. Greco and Y. Tor, *Chem. Rev.*, 2010, **110**, 2579; (f) J. Wu, W. Liu, J. Ge, H. Zhang and P. Wang, *Chem. Soc. Rev.*, 2011, **40**, 3483.
- (a) D. Maity and T. Govindaraju, *Inorg. Chem.*, 2010, **49**, 7229; (b) S. Sen, T. Mukherjee, B. Chattopadhyay, A. Moirangthem, A. Basu, J. Marek and P. Chattopadhyay, *Analyst*, 2012, **137**, 3975; (c) S. Sinha, R. R. Koner, S. Kumar, J. Mathew, P. V. Monisha, I. Kazi and S. Ghosh, *RSC Adv.*, 2013, **3**, 345; (d) C.-H. Chen, D.-J. Liao, C.-F. Wan and A.-T. Wu, *Analyst*, 2013, **138**, 2527; (e) W.-H. Ding, W. Cao, X.-J. Zheng, D.-C. Fang, W.-T. Wong and L.-P. Jin, *Inorg. Chem.*, 2013, **52**, 7320; (f) X. Shi, H. Wang, T. Han, X. Feng, B. Tong, J. Shi, J. Zhi and Y. Dong, *J. Mater. Chem.*, 2012, **22**, 19296; (g) S. Samanta, B. Nath and J. B. Baruah, *Inorg. Chem. Commun.*, 2012, **22**, 98; (h) Q. Meng, H. Liu, S. Cheng, C. Cao and J. Ren, *Talanta*, 2012, **99**, 464; (i) A. Sahana, A. Banerjee, S. Lohar, B. Sarkar, S. K. Mukhopadhyay and D. Das, *Inorg. Chem.*, 2013, **52**, 3627; (j) H. M. Park, B. N. Oh, J. H. Kim, W. Qiong, I. H. Hwang, K.-D. Jung, C. Kim and J. Kim, *Tetrahedron Lett.*, 2011, **52**, 5581; (k) D. Maity and T. Govindaraju, *Chem. Commun.*, 2012, **48**, 1039; (l) K. K. Upadhyay and A. Kumar, *Org. Biomol. Chem.*, 2010, **8**, 4892; (m) A. Sahana, A. Banerjee, S. Lohar, A. Banik, S. K. Mukhopadhyay, D. A. Safin, M. G. Babashkina, M. Bolte, Y. Garcia and D. Das, *Dalton Trans.*, 2013, **42**, 13311.
- (a) S. Sharma, M. S. Hundal and G. Hundal, *Org. Biomol. Chem.*, 2013, **11**, 654; (b) S. Sharma, M. S. Hundal and G. Hundal, *Tetrahedron Lett.*, 2013, **54**, 2423; (c) S. Sharma, M. S. Hundal, N. Singh and G. Hundal, *Sens. Actuators, B*, 2013, **188**, 590; (d) V. K. Bhardwaj, S. Sharma, N. Singh, M. S. Hundal and G. Hundal, *Supramol. Chem.*, 2011, **23**, 790.
- (a) D. Luneau and C. Evans, *J. Chem. Soc., Dalton Trans.*, 2002, 83; (b) A. Koll, *Int. J. Mol. Sci.*, 2003, **4**, 434.
- W. Rodriguez-Cordoba, J. S. Zugazagoitia, E. Collado-Fregoso and J. Peon, *J. Phys. Chem. A*, 2007, **111**, 6241.
- (a) R. Martínez-Mañez and F. Sancenòn, *Chem. Rev.*, 2003, **103**, 4419; (b) V. K. Bhardwaj, A. P. S. Pannu, N. Singh, M. S. Hundal and G. Hundal, *Tetrahedron*, 2008, **64**, 5384; (c) J. Shao, Y. H. Qiao, H. Lin and H. K. Lin, *J. Lumin.*, 2008, **128**, 1985; (d) L. Prodi, F. Bolletta, M. Montalti and N. Zaccheroni, *Coord. Chem. Rev.*, 2000, **205**, 59.
- (a) J. N. Demas and G. A. Crosby, *J. Phys. Chem.*, 1971, **75**, 991; (b) R. G. LeBEL and D. A. I. GORING, *J. Chem. Eng. Data*, 1962, **7**, 100.
- (a) A. Helal, S. H. Lee, S. H. Kim and H.-S. Kim, *Tetrahedron Lett.*, 2010, **51**, 3531; (b) L. Qu, C. Yin, F. Huo, Y. Zhang and Y. Li, *Sens. Actuators, B*, 2013, **183**, 636.
- P. Job, *Ann. Chim.*, 1928, **9**, 113.
- H. A. Benesi and J. H. Hildebrand, *J. Am. Chem. Soc.*, 1949, **71**, 2703.
- A. Caballero, R. Martínez, V. Lloveras, I. Ratera, J. Vidal-Gancedo, K. Wurst, A. Tárraga, P. Molina and J. Veciana, *J. Am. Chem. Soc.*, 2005, **127**, 15666.
- (a) S. Goswami and R. Chakrabarty, *Tetrahedron Lett.*, 2009, **50**, 5994; (b) M. C. Davis, *Synth. Commun.*, 2007, **37**, 1457.